A Compton scattering study on the Hume-Rothery mechanism of AlCu–TM (TM: transition metal) quasicrystals

2006 J. Phys.: Condens. Matter 18 7203

(http://iopscience.iop.org/0953-8984/18/31/015)

INSTITUTE OF PHYSICS PUBLISHING JOURNAL OF PHYSICS: CONDENSED MATTER

J. Phys.: Condens. Matter **18** (2006) 7203–7208 doi:10.1088/0953-8984/18/31/015

A Compton scattering study on the Hume-Rothery mechanism of AlCu–TM (TM: transition metal) quasicrystals

J T Okada[1,4], Y Sakurai[2], Y Watanabe[1], R Ishikawa[1], Y Yokoyama[3], N Hiraoka[2], M Itou[2] and S Nanao[1]

[1] Institute of Industrial Science, The University of Tokyo, Meguro 153-8505, Japan
[2] Japan Synchrotron Radiation Research Institute (JASRI), SPring-8, Sayo, Hyogo 679-5198, Japan
[3] Institute for Materials Research, Tohoku University, Sendai 980-8577, Japan
[4] Department of Advanced Materials Science, The University of Tokyo, Kiban-toh 502, 5-1-5 Kashiwanoha, Kashiwa-shi, Chiba 277-8561, Japan

E-mail: jt.okada@phys.mm.t.u-tokyo.ac.jp

Received 31 March 2006, in final form 27 June 2006
Published 21 July 2006
Online at stacks.iop.org/JPhysCM/18/7203

Abstract

The electron momentum distributions in icosahedral $Al_{64}Cu_{23}Fe_{13}$, icosahedral $Al_{63}Cu_{23}Ru_{13}$ and decagonal $Al_{65}Cu_{15}Co_{20}$ quasicrystals have been studied using the high-resolution Compton scattering technique. The electron-per-atom ratios (e/a) of the quasicrystals were determined quantitatively for the first time from the Compton profiles. The radii of the Fermi spheres were evaluated from the values of e/a on the basis of the free-electron model. Comparisons between the radius of the Fermi spheres and the size of the quasi-Brillouin zones show that the icosahedral quasicrystals meet the empirical matching condition, while the decagonal quasicrystal does not do this so well. This implies that the Hume-Rothery mechanism works for the formation of the pseudogap near the Fermi level in the icosahedral quasicrystals, although it operates only slightly in the decagonal quasicrystal.

Quasicrystals (QCs) were discovered in 1984 [1] as a new solid-state phase, possessing the new long-range order, quasiperiodicity. The discovery initiated an intensive search for new QCs in order to confirm the universality of the quasiperiodic lattice in condensed matter. Already, several kinds of QCs with different rotational and translational symmetries have been found in various alloys, and some of them have been reported to be thermodynamically stable phases [2]. The stable QCs with icosahedral (i-)symmetry have been considered as Hume-Rothery electron compounds, since almost all the stable i-QCs form in a certain range of electron-per-atom ratio, e/a. It was soon pointed out theoretically that the existence of a pseudogap contributes to

the stabilization of QCs [3]. The pseudogap forms in the density of states across the Fermi level E_F in two possible ways; one is by the interaction between the quasi-Brillouin zone (q-BZ) boundary and the Fermi sphere (FS), i.e., the Hume-Rothery mechanism (HRM), and the other is by sp–d hybridization. When the Fermi energy is in the pseudogap, one can expect a reduction of the total band energy. The HRM works most effectively in i-QCs since the q-BZs possess nearly spherical symmetry. In Al–transition metal (TM) QCs, the d states of a TM element are strongly hybridized with the s and p states of Al. The sp–d hybridization further deepens and widens the pseudogap formed by the q-BZ–FS interaction. The deep pseudogap in the vicinity of E_F contributes to the stabilization of the i-QCs. Experimentally, the importance of the sp–d hybridization in forming the pseudogap has been confirmed by photoemission spectroscopy and soft x-ray emission and absorption spectroscopy [4]. Regarding the HRM, however, its additional contribution to the pseudogap opening still remains unclear because of limits of experimental methods which directly caliper the Fermi surface.

The diameter of the FS has been estimated from the value of e/a on the basis of the free-electron model [2]. The empirical value of 1.75 for Al–Cu–TM QCs gives the diameter of the FS which corresponds to intense Bragg diffraction spots. The value of e/a for Al–Cu–TM QCs, however, has not been evaluated experimentally. In this work, we have studied the Compton profiles of i-$Al_{64}Cu_{23}Fe_{13}$, i-$Al_{63}Cu_{23}Ru_{13}$ and decagonal (d-)$Al_{65}Cu_{15}Co_{20}$, obtained by the high-resolution Compton scattering technique. By analysing the valence-electron part of the Compton profiles, the values of e/a have been obtained quantitatively for the first time.

In a Compton scattering experiment, one can obtain the so-called Compton profile,

$$J(p_z) = \int\int n(\mathbf{p})\,\mathrm{d}p_x\,\mathrm{d}p_y, \tag{1}$$

where $n(\mathbf{p})$ is the ground-state electron momentum density. In an independent-particle model, the momentum density is given by

$$n(\mathbf{p}) = \sum_i |\psi_i(\mathbf{r})\exp(\mathrm{i}\mathbf{p}\cdot\mathbf{r})\,\mathrm{d}\mathbf{r}|^2, \tag{2}$$

where $\psi_i(\mathbf{r})$ is an electron wavefunction. The summation in equation (2) extends over all the occupied states. The area under the Compton profile gives the total number of electrons N,

$$\int_{-\infty}^{\infty} J(p_z)\,\mathrm{d}p_z = N. \tag{3}$$

When the profile is decomposed into two or more components reflecting different electronic states, the area under each component gives the number of electrons occupying that state.

Until now, the Compton scattering technique has been applied to i-Al_6Li_3Cu [5], d-$Al_{72}Ni_{12}Co_{16}$ [6] and i-$Cd_{84}Yb_{16}$ QCs [7]. In all cases, a partial profile with a parabola-like shape has been observed in the valence-electron Compton profiles. The partial profiles are isotropic and thus are well accounted for by the free-electron-like sp bands. The diameter of the Fermi sphere has been estimated from the number of electrons under the parabola-like partial profile. Comparing the sizes between the FSs and the q-BZs, it has been concluded that the HRM works effectively in i-Al_6Li_3Cu and does not do this so well for d-$Al_{72}Ni_{12}Co_{16}$, while both the HRM and the sp–d hybridization play important roles in forming a deep pseudogap in i-$Cd_{84}Yb_{16}$.

Single grains of d-$Al_{65}Cu_{15}Co_{20}$ (d-AlCuCo) and i-$Al_{64}Cu_{23}Fe_{13}$ (i-AlCuFe) grown by the Czochralski method and polycrystalline samples of i-$Al_{63}Cu_{23}Ru_{13}$ (i-AlCuRu) were used for Compton scattering measurements. The Compton scattering experiment was carried out at BL08W, SPring-8 [8]. The reader is referred to the report of Hiraoka *et al* [9] for the details of the spectrometer. The energy of the incident x-rays was 116 keV and the scattering angle

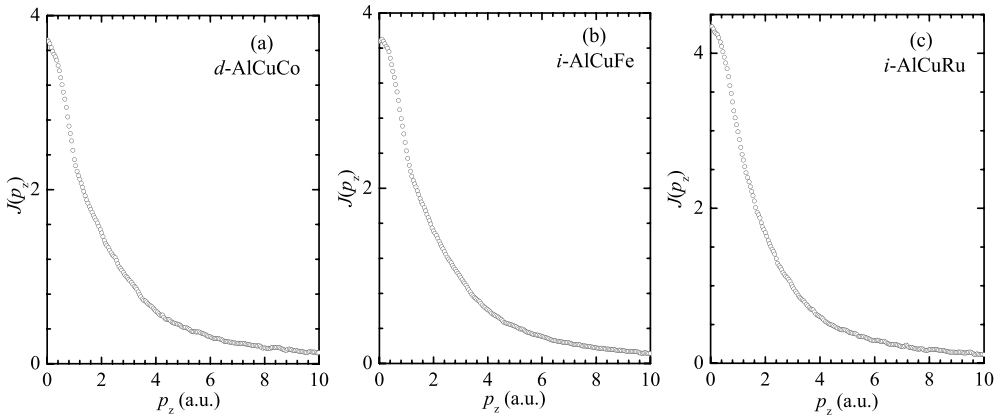

Figure 1. Experimental Compton profile of total electrons; (a) d-$Al_{65}Cu_{15}Co_{20}$, (b) i-$Al_{64}Cu_{23}Fe_{13}$ and (c) i-$Al_{63}Cu_{23}Ru_{13}$.

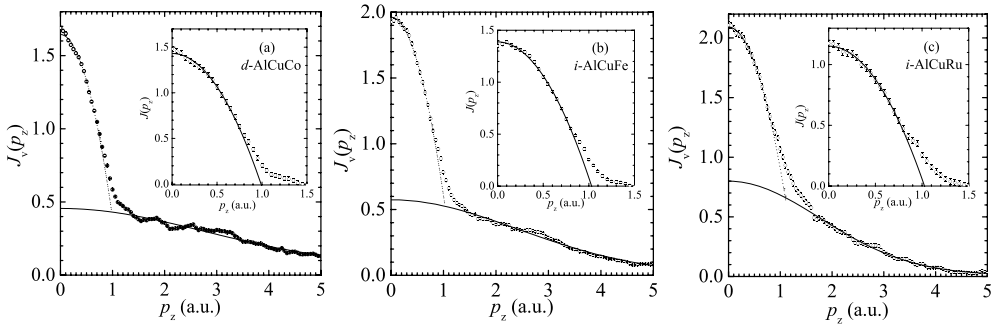

Figure 2. Experimental valence-electron Compton profile $J_v(p_z)$; (a) d-$Al_{65}Cu_{15}Co_{20}$, (b) i-$Al_{64}Cu_{23}Fe_{13}$ and (c) i-$Al_{63}Cu_{23}Ru_{13}$. The insets show the inverted parabola-like part of the profile, which is obtained by subtracting the Gaussian-like part from the valence-electron profile.

was 165°. The energy spectra of Compton-scattered x-rays were measured at room temperature along the [00002] directions for d-AlCuCo and [111000] for i-AlCuFe, where the index defined by Yamamoto and Ishihara [10] is used. The experimental momentum resolution was 0.16 atomic units (au). The data processing used to deduce the Compton profile from the raw energy spectrum consists of the following procedures: background subtraction; and energy-dependent corrections for the Compton scattering cross section, the absorption of incident and scattered x-rays in the sample, the efficiency of the analyser and the detector, and the double scattering.

Figure 1 shows the measured total-electron Compton profiles of d-AlCuCo, i-AlCuRu and i-AlCuFe. By subtracting the theoretical core-electron profile $J_c(p_z)$, the valence-electron Compton profile $J_v(p_z)$ is obtained. The core-electron profile of each state is obtained from the theoretical data based on the free-atom Hartree–Fock calculations by Biggs *et al* [11], where $(1s)^2(2s)^2(2p)^6$ for Al, $(1s)^2(2s)^2(2p)^6(3s)^2(3p)^6$ for Cu and Co, and $(1s)^2(2s)^2(2p)^6(3s)^2(3p)^6(4s)^2(4p)^6$ for Ru are treated as the core electrons. The experimental $J_v(p_z)$ consists of two distinct parts as shown in figure 2: one is an inverted parabola-like part in the region of $|p_z| < 1.0$ au and the other is a broad Gaussian-like part. The Gaussian-like part resembles the profile of the TM d electrons in terms of the width of the profile.

There is experimental and theoretical evidence that strong sp–d hybridization affects the electronic structure near E_F. The sp–d hybridization can be written as $|sp + d|^2 =$

$|\mathrm{sp}|^2+2|\mathrm{sp}*\mathrm{d}|+|\mathrm{d}|^2$, where $|\mathrm{sp}|^2$ and $|\mathrm{d}|^2$ are the sp electrons' and d electrons' terms [12]. The $|\mathrm{sp}|^2$ and $|\mathrm{d}|^2$ parts are observed as parabola-like and Gaussian-like profiles, respectively. The $2|\mathrm{sp}*\mathrm{d}|$ part is the interference term, which brings about directionally dependent oscillations in momentum density and thus directional anisotropy in Compton profiles. In this work, we assume that the interference terms are negligibly small compared to the sp and d electrons' terms since the observed directional anisotropies in Compton profiles are small.

The insets of figure 2 show the inverted parabola-like parts of d-AlCuCo, i-AlCuFe and i-AlCuRu, which are obtained by subtracting the Gaussian-like parts from the valence-electron profiles. The Gaussian-like parts represent 3d or 4d electrons from Cu, Co, Fe or Ru. The previous experiments show that a Gaussian is a good approximation to the partial profile from d electrons [6, 7]. In the present analysis, a Gaussian was fitted to the valence-electron profile in the range between $p_z = 1.5$ and $p_z = 5.0$ au. In the insets of figure 2, the overall shape of profiles can be reproduced by an inverted parabola (solid line) in the range from $p_z = 0$ to 0.90 au, although a tail is observed in the experimental profiles at momenta larger than $p_z = 0.90$ au. In an electron-gas model, the electron–electron interaction produces a tail beyond the Fermi momentum in a Compton profile [13] and the electron–lattice interaction makes an addition to the tail with high-momentum components centred at reciprocal points due to the Umklapp processes [14]. Therefore, we evaluate the value of e/a by integrating the inverted part between $p_z = 0$ and 1.5 au.

The area under the inverted part between $p_z = 0$ and 1.5 au gives $e/a = 2.00 \pm 0.08$ for d-AlCuCo, 2.00 ± 0.08 for i-AlCuFe and 1.85 ± 0.09 for i-AlCuRu. The present values of e/a are slightly larger than the phenomenological value of 1.75 for AlCu–TM QCs calculated using Raynor's valency [2]. From the value of e/a, the radius of the Fermi sphere, k_F, is calculated to be 0.86 ± 0.01 au for d-AlCuCo, 0.86 ± 0.01 au for i-AlCuFe and 0.80 ± 0.01 au for i-AlCuRu using the relation between k_F and the number of electrons n: $k_\mathrm{F} = (3\pi^2 n)^{1/3}$.

Figure 3 shows the x-ray powder diffraction patterns and the positions of k_F for the three QCs. The position of k_F for i-AlCuRu is between the dominant (222100) and (221001) diffraction peaks and that for i-AlCuFe is very close to the (221001) peak. The q-BZs defined by the (222100) and (221001) planes are icosahedral polyhedra, that are very close to a sphere. This finding suggests that the HRM works in the icosahedral AlCuRu and AlCuFe QCs. On the other hand, the d-AlCuCo QC shows that the k_F is larger than the size of the inscribed sphere of the q-BZ defined by the dominant (00002) planes. In addition, the q-BZ defined by the strong diffraction planes that appeared at around 0.8 au is a polyhedron that differs from a sphere. These findings suggest that the HRM does not contribute much to the formation of the pseudogap in the decagonal AlCuCo QC, compared with that in the icosahedral AlCuRu and AlCuFe QCs. This conclusion is consistent with the previous work on the decagonal AlNiCo QC, in which the evaluated k_F is also larger than the size of the inscribed sphere of the q-BZ [6].

In summary, the Compton profiles of d-$Al_{65}Cu_{15}Co_{20}$, i-$Al_{64}Cu_{23}Fe_{13}$ and i-$Al_{63}Cu_{23}Ru_{13}$ have been measured using the high-resolution Compton scattering spectrometer at BL08W, SPring-8. The experimental valence-electron Compton profiles have been decomposed into two components, an inverted parabola-like part and a broad Gaussian-like one. The electron-per-atom ratio, e/a, has been evaluated from the area under the inverted parabola-like part, and it is found that the experimental values of e/a are in reasonable agreement with the phenomenological value calculated using Raynor's valency, although the experimental values are slightly larger than the phenomenological value. The Fermi spheres of i-AlCuRu and i-AlCuFe overlap with the main quasi-Brillouin zone boundaries, while that of d-AlCuCo does not overlap as much. This finding indicates that the Hume-Rothery mechanism works for the formation of the pseudogap in the icosahedral QCs, but operates only slightly in the decagonal QCs.

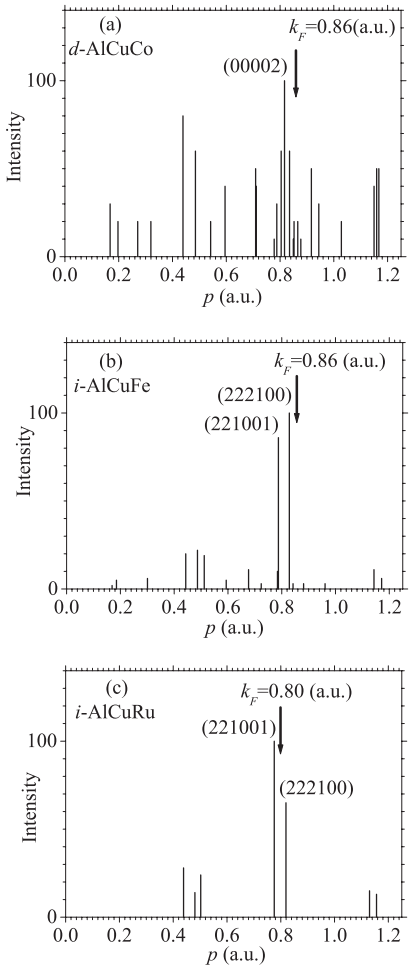

Figure 3. Experimental data from x-ray powder diffraction, which show the relationship between the position of the FS (k_F) and the dominant Bragg diffraction planes.

Acknowledgments

We are grateful to Professor Kaoru Kimura for illuminating discussions. The Compton profile measurements were performed with the approval of JASRI (Proposal No 2002A 0436-ND-np. This work was supported in part by a Grant-in-Aid from the Ministry of Education, Culture, Sports, Science and Technology of Japan, Iketani Science and Technology Foundation, and the Light Metal Educational Foundation, Incorporated.

References

[1] Shechtman D, Blech I, Gratias D and Cahn J W 1983 *Phys. Rev. Lett.* **53** 1951
[2] Stadnik Z M 1999 *Physical Properties of Quasicrystals* (*Springer Series in Solid-State Sciences* vol 126) (Berlin: Springer)
[3] Smith A P and Ashcroft N W 1987 *Phys. Rev. Lett.* **59** 1365

[4] Stadnik Z M, Purdie D, Garnier M, Baer Y, Tsai A P, Inoue A, Edagawa K, Takeuchi S and Buschow K H J 1997 *Phys. Rev.* B **55** 10938
[5] Tanaka Y, Sakurai Y, Nanao S, Shiotani N, Ito M, Sakai N, Kawata H and Iwazumi T 1994 *J. Phys. Soc. Japan* **63** 3349
[6] Okada J T, Watanabe Y, Yokoyama Y, Hiraoka N, Itou M, Sakurai Y and Nanao S 2002 *J. Phys.: Condens. Matter* **14** L43
[7] Okada J T, Watanabe Y, Nanao S, Tamura R, Takeuchi S, Yokoyama Y, Hiraoka N, Itou M and Sakurai Y 2003 *Phys. Rev.* B **68** 132204
[8] Sakurai Y 1998 *J. Synchrotron Radiat.* **5** 208
[9] Hiraoka N, Itou M, Ohata T, Mizumaki M, Sakurai Y and Sakai N 2001 *J. Synchrotron Radiat.* **8** 26
[10] Yamamoto A and Ishihara K N 1988 *Acta Crystallogr.* A **44** 707
[11] Biggs F, Mendelsohn L B and Mann J B 1975 *At. Data Nucl. Data Tables* **16** 201
[12] Weyrich W, Pattisons P and Williams B G 1979 *Chem. Phys.* **41** 271
[13] Daniel E and Vosko H 1960 *Phys. Rev.* **120** 2041
[14] Eisenberger P, Lam L, Platzman P M and Schmidt P 1972 *Phys. Rev.* B **10** 3671